# Supporting Information

## Stabilization of hairpins and bulged secondary structures of nucleic acids by single incorporation of α,β-D-CNA featuring a gauche(+) alpha torsional angle

**Béatrice Gerland, Pierre Millard, Christelle Dupouy, Brice-Loïc Renard and Jean-Marc Escudier *[a]**

Laboratoire de Synthèse et Physico-Chimie de Molécules d'Intérêt Biologique, UMR 5068 CNRS, Université Paul Sabatier, 118 Route de Narbonne, 31062 Toulouse Cedex 9 (France)

[*] fax: (+33)5-6155-6011
E-mail: escudier@chimie.ups-tlse.fr

**CONTENTS**

**Synthesis of ($S_C$, $R_P$)-α,β-D-CNA TT phosphoramidite**

**General Methods**. Reactions were conducted under an atmosphere of argon when anhydrous solvents were used. All solvents were distilled and dried before use. All reagents were obtained from commercial suppliers and were used without further purification. Products were purified by medium pressure liquid chromatography apparatus through 15 µm silica. $CDCl_3$ was used as NMR solvent as well as internal standards for $^{13}C$ and $^{31}P$ NMR.

**5'-*O*-dimethoxytrityl-3'-*O*-(cyanoethyl-diisopropylaminophosphoramidite)-α,β-D-CNA ($S_C$, $R_P$).**

To a solution of **5'-*O*-dimethoxytrityl 3'-OH-α,β-D-CNA ($S_C$, $R_P$)** [1] (920 mg, 1.06 mmol) in anhydrous THF (10 mL) were added at room temperature under an argon atmosphere, diisopropylethylamine (732 µL, 4.24 mmol) and (2-cyanoethyl)(*N*,*N*-diisopropylamino)-chlorophosphite (500 mg, 2.12 mmol). After 30 min of stirring the *N*,*N*-diisopropylethylamine hydrochloride was filtered off and the reaction mixture was diluted with ethyl acetate saturated with argon. The organic layer was washed with a cold aqueous solution of $K_2CO_3$ 10%, dried over $MgSO_4$ and the solvent was removed under reduced pressure. The crude material was submitted to silica gel chromatography with ethyl acetate/$Et_3N$ 1% as eluent. The α,β-D-CNA phosphoramidite (1.07 g, 1.0 mmol, 95% yield) was recovered (mixtures of diastereoisomers) as a white foam after careful removal of the solvent under high vacuum for 24 h. TLC, $R_f$ (AcOEt, 1% $Et_3N$) = 0.20. $^{13}C$ NMR (75 MHz, $CDCl_3$) $\delta_{ppm}$ 164.0; 163.9; 158.8; 150.8; 150.7; 150.6; 144.0; 136.4; 135.1; 135.0; 130.1; 128.1; 128.0; 127.3; 121.2; 118.1; 117.8; 113.3; 111.9; 111.3; 87.3; 86.5; 86.1; 85.9; 80.0; 79.6; 79.5; 78.9; 78.8; 72.9; 72.7; 72.5; 68.4; 63.4; 60.4; 58.4; 58.3; 58.2; 58.1; 57.8; 57.7; 5.3; 45.3; 38.8; 38.5; 38.2; 29.7; 28.1; 24.6; 24.5; 24.4; 22.9; 22.8; 21.4; 20.5; 20.4; 20.1; 20.0; 12.5; 11.6. $^{31}P$ NMR (81 MHz, $CDCl_3$) $\delta_{ppm}$ 149.2; 147.8; -8.3; -8.8. MS (electrospray): 1075.5 ([M+$H^+$]$^+$); 1097.5 ([M+$Na^+$]$^+$); 1113.0 ([M+$K^+$]$^+$).

[1] I. Le Clezio, J-M Escudier, A. Vigroux, *Org. Lett*. 2003, **5**, 161-164.

## Oligonucleotides synthesis

The oligonucleotides were assembled on CPG support (1 or 0.2 μmol scale) on a PerSeptive Biosystems, 8909 Expedite or an ABI 394 using the standard phosphoramidite chemistry or purchased from Eurogentec corp. when unmodified. After complete assembly of the oligonucleotide chain, deprotections were achieved with $NH_4OH$ (33%) at 25 °C for 24 h. The crude product was analysed and purified by reversed phase HPLC (Kromasil $C_{18}$, 7 μm, 100 Å, 250 x 4.6 mm for analysis or 250 x 20 mm for purification scale) on a Waters apparatus (600 E pomp system controller and a 996 photodiode array detector), using a gradient from 95% of A to 70% of A in B (A: TEAA buffer 0.05 M, pH 7.0; B: $CH_3CN$). Analysis of the oligonucleotides was performed by mass spectrometry in MALDI TOF mode on a PerSeptive Biosystems Voyager Spectrometer or a Waters Micromass MX with THAP, 10% ammonium citrate as matrix.

***Table S1*** : MALDI-TOF-MS of oligonucleotides containing ($S_C$, $R_P$) α,β-D-CNA TT.

| Entry | Name | Sequence | MW calculated | MW found |
|---|---|---|---|---|
| **1** | $^{6}H_{AT}T_5$ | ATCCTA*TTTTT*TAGGAT | 5165.4 | 5159.1 |
| **2** | $^{6}H_{AT}T_5gp_1$ | ATCCTA***TT****TTT*TAGGAT | 5191.6 | 5186.2 |
| **3** | $^{6}H_{AT}T_5gp_2$ | ATCCTA*T****TT****TT*TAGGAT | 5191.6 | 5187.2 |
| **4** | $^{6}H_{AT}T_5gp_3$ | ATCCTA*TT****TT****T*TAGGAT | 5191.6 | 5190.4 |
| **5** | $^{6}H_{AT}T_5gp_4$ | ATCCTA*TTT****TT***TAGGAT | 5191.6 | 5189.6 |
| **6** | $^{6}H_{AT}T_5gp_5$ | ATCCTA*TTTT****TT***AGGAT | 5191.6 | 5188.9 |
| **7** | $^{7}H_{CG}T_5$ | AGGATCC*TTTTT*GGATCCT | 5784.8 | 5783.3 |
| **8** | $^{7}H_{CG}T_5gp_1$ | AGGATCC***TT****TTT*GGATCCT | 5810.3 | 5810.2 |
| **9** | $^{7}H_{CG}T_5gp_2$ | AGGATCC*T****TT****TT*GGATCCT | 5810.3 | 5811.1 |
| **10** | $^{7}H_{CG}T_5gp_3$ | AGGATCC*TT****TT****T*GGATCCT | 5810.3 | 5807.4 |
| **11** | $^{7}H_{CG}T_5gp$ | AGGATCC*TTT****TT***GGATCCT | 5810.3 | 5807.3 |
| **12** | $^{6}H_{CG}T_4$ | GGATCC*TTTT*GGATCC | 4863.2 | 4861.4 |
| **13** | $^{6}H_{CG}T_4gp_2$ | GGATCC*T****TT****T*GGATCC | 4888.7 | 4886.5 |
| **14** | $^{6}H_{CG}T_4gp_3$ | GGATCC*TT****TT***GGATCC | 4888.7 | 4886.6 |
| **15** | $^{5}H_{CG}T_4$ | GATCC*TTTT*GGATC | 4244.8 | 4244.0 |
| **16** | $^{5}H_{CG}T_4gp_2$ | GATCC*T****TT****T*GGATC | 4270.3 | 4269.6 |

| | | | | |
|---|---|---|---|---|
| **17** | $^{5}H_{CG}T_4gp_3$ | GATCC*TT**TT***GGATC | 4270.3 | 4269.7 |
| **18** | $^{4}H_{CG}T_4$ | ATCC*TTTT*GGAT | 3626.4 | 3625.6 |
| **19** | $^{4}H_{CG}T_4gp_2$ | ATCC*T**TT**T*GGAT | 3649.9 | 3646.2 |
| **20** | $^{4}H_{CG}T_4gp_3$ | ATCC*TT**TT***GGAT | 3649.9 | 3647.7 |
| **21** | $^{3}H_{CG}T_4$ | TCC*TTTT*GGA | 3009.9 | 3006.8 |
| **22** | $^{3}H_{CG}T_4gp_2$ | TCC*T**TT**T*GGA | 3035.4 | 3032.9 |
| **23** | $^{3}H_{CG}T_4gp_3$ | TCC*TT**TT***GGA | 3035.4 | 3033.4 |
| **24** | $^{2}H_{CG}T_4$ | CC*TTTT*GG | 2391.6 | 2389.5 |
| **25** | $^{2}H_{CG}T_4gp_2$ | CC*T**TT**T*GG | 2417.1 | 2414.3 |
| **26** | $^{2}H_{CG}T_4gp_3$ | CC*TT**TT***GG | 2417.1 | 2415.2 |
| **27** | Bulge | GATTTGCATA**TT**CATGAG | 5555.7 | 5555.0 |

## Thermal denaturation studies

Absorbance versus temperature profiles were recorded at 260 nm in fused quartz cuvettes on a Carry 300 Bio spectrophotometer equipped with a Peltier temperature control device. Each sample was heated to 90°C and then slowly cooled before measurements. The temperature is increased by 0.5°C/min from 15 to 90°C. The strand was in 3.5 to 5 µM range concentration (10 mM phosphate buffer, pH 7.00, 100 mM NaCl, 1 mM EDTA) assuming identical extinction coefficient for the α,β-D-CNA including oligonucleotide and the corresponding unmodified ones. Melting temperatures were calculated by use of the Carry software.

***Figure S1.*** Thermal denaturation curves (Table 2, entry 1 to 6), for hairpins 5'-d(ATCCTA*TTTTT*TAGGAT) with five variable positions of the α,β-D-CNA TT featuring the alpha *gauche*(+) conformation within the loop.

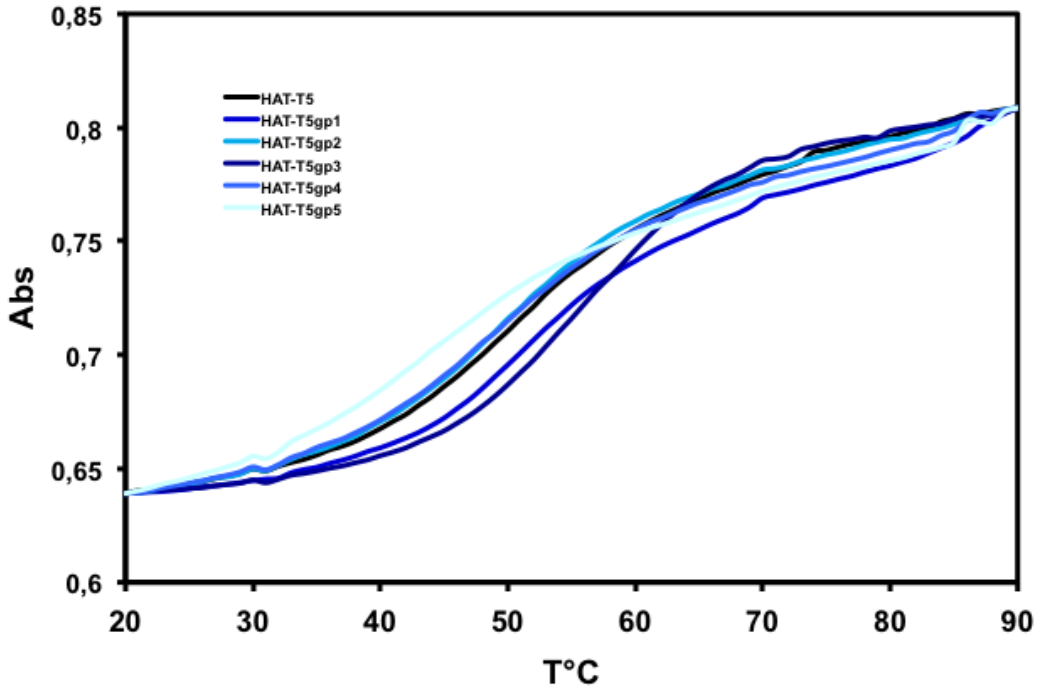


***Figure S2.*** Thermal denaturation curves (Table 2, entry 7 to 11), for hairpins 5'-d(AGGATCC*TTTTT*GGATCCT) with four variable positions of the α,β-D-CNA TT featuring the alpha *gauche*(+) conformation within the loop.

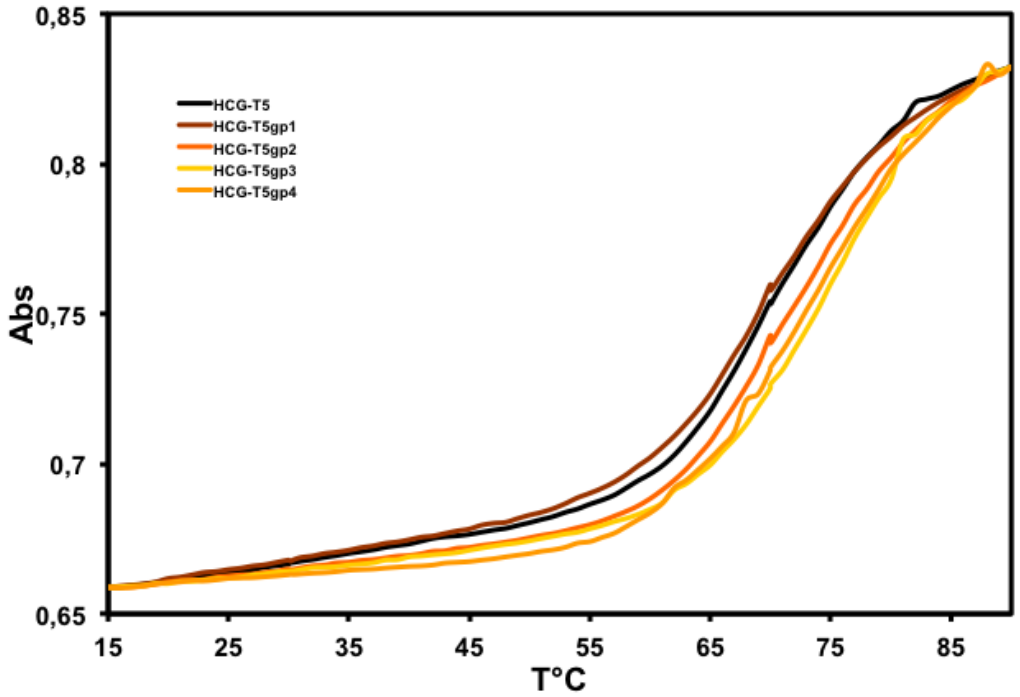


***Figure S3.*** Tm *vs* ln[NaCl] plots, for hairpins 5'-d(ATCCTA*TTTTT*TAGGAT) with five variable positions of the α,β-D-CNA TT featuring the alpha *gauche*(+) conformation within the loop.

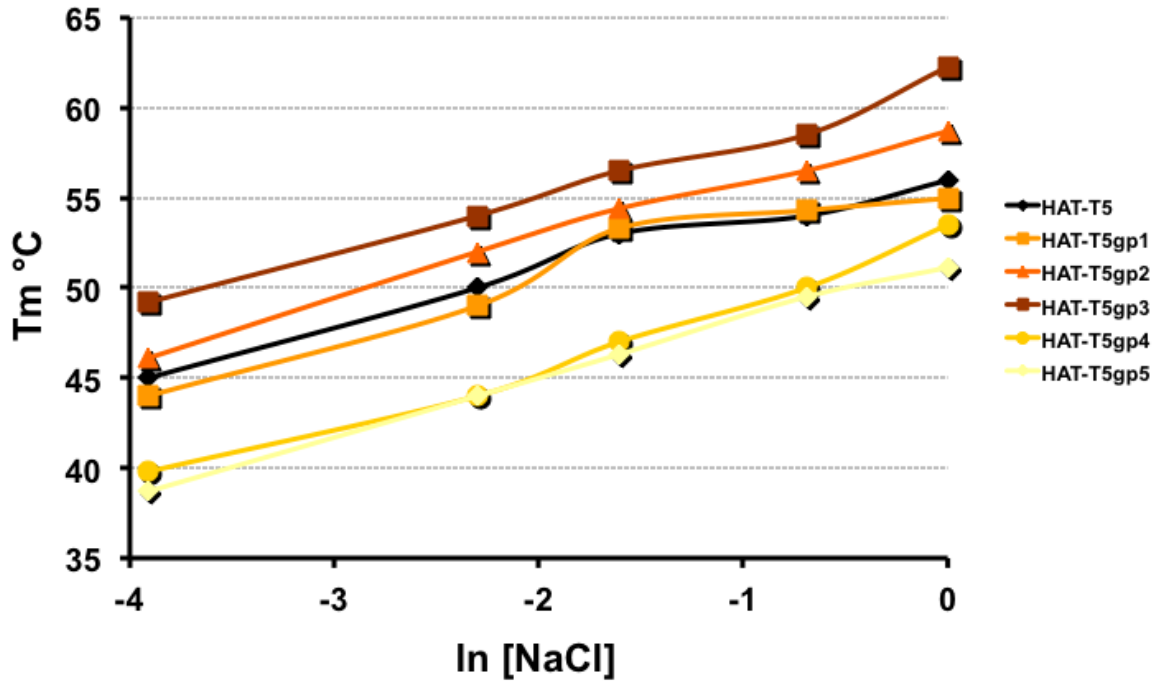


***Figure S4.*** Tm *vs* ln[NaCl] plots, for hairpins 5'-d(AGGATCC*TTTTT*GGATCCT) with four variable positions of the α,β-D-CNA TT featuring the alpha *gauche*(+) conformation within the loop.

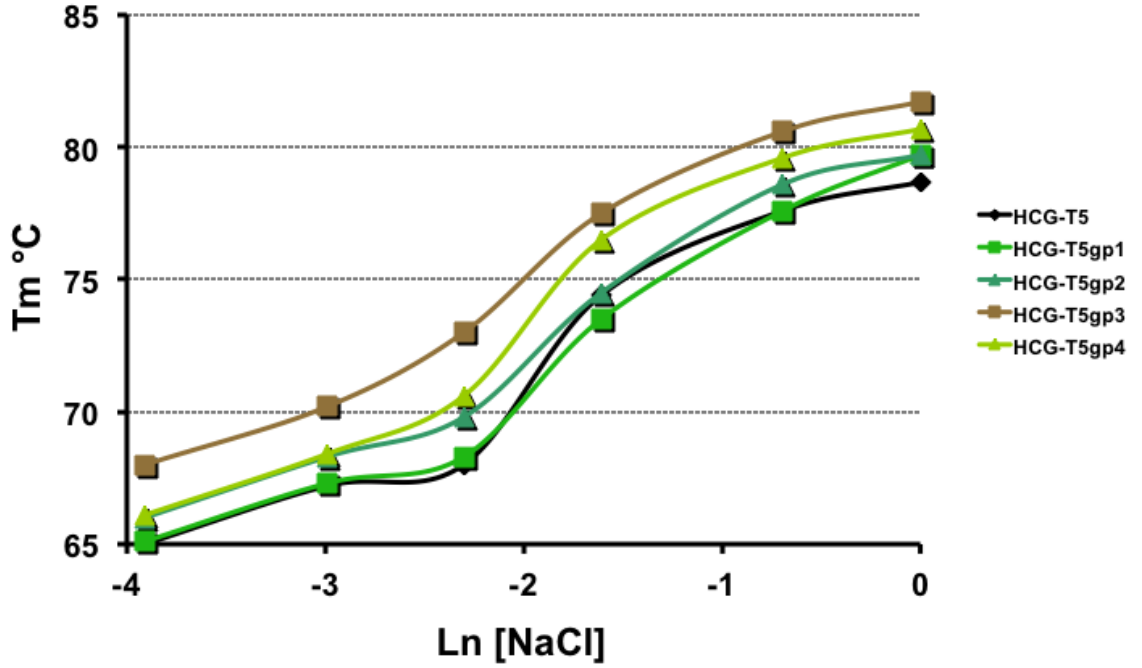


***Figure S5.*** CD spectra of hairpins 5'-d(ATCCTA*TTTTT*TAGGAT) with five variable positions of the α,β-D-CNA TT featuring the alpha *gauche*(+) conformation within the loop (Table 1, entry 10 to 15), in sodium phosphate buffer (10 mM, pH 7.0), NaCl (100 mM), and EDTA (1 mM); T = 25°C. Strand concentration = 5 μM.

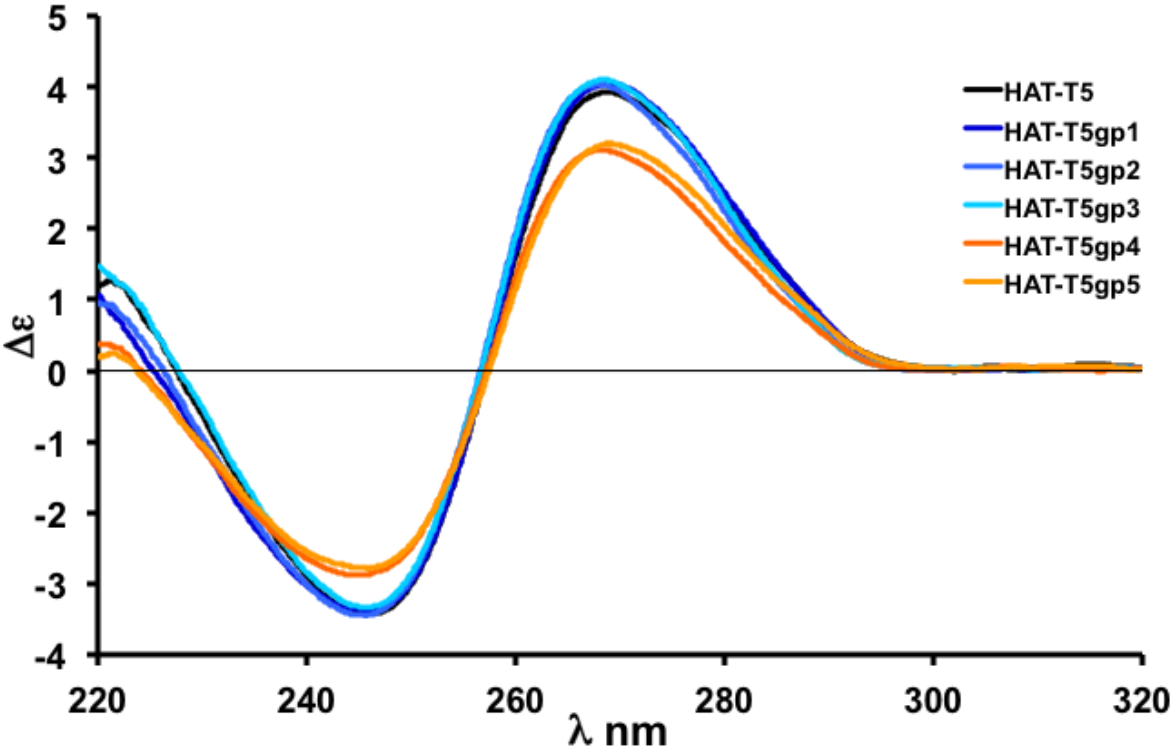

***Figure S6.*** CD spectra of hairpins 5'-d(AGGATCC*TTTTT*GGATCCT) with four variable positions of the α,β-D-CNA TT featuring the alpha *gauche*(+) conformation within the loop (Table 1, entry 16 to 20), in sodium phosphate buffer (10 mM, pH 7.0), NaCl (100 mM), and EDTA (1 mM); T = 25°C. Strand concentration = 5 μM.

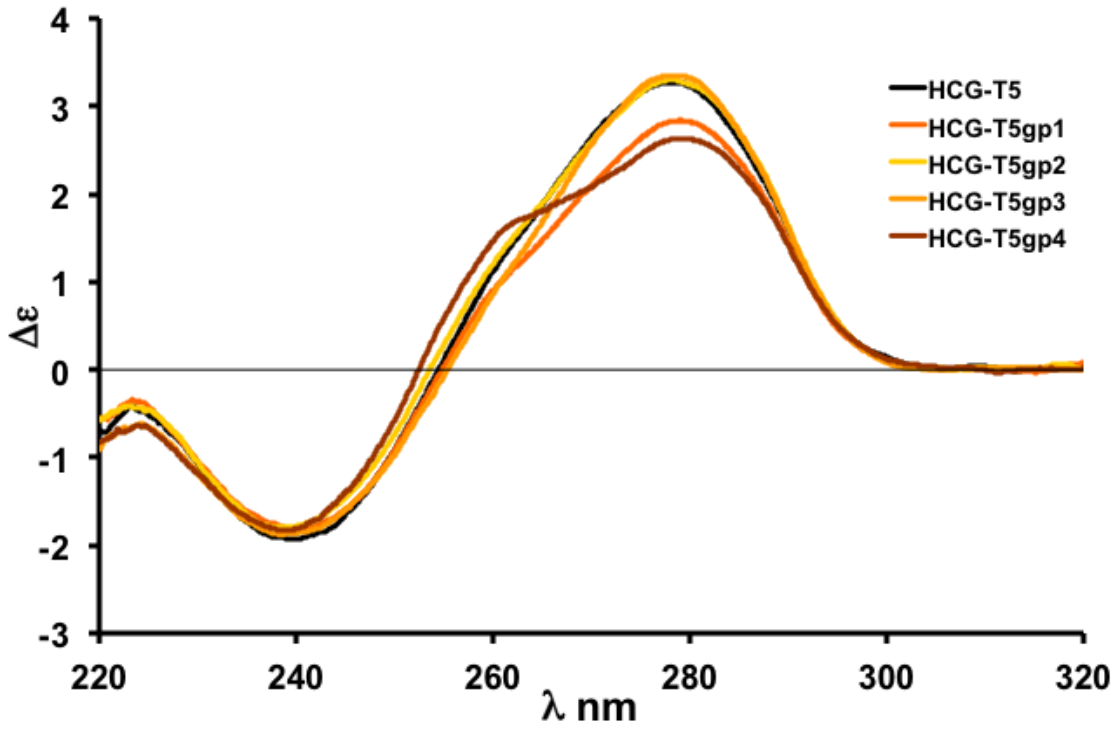


***Figure S7.*** CD spectra at T = 90°C of hairpins $^{i}H_{CG}T_4$ with stem composed from two to six base pairs ($2 \leq i \leq 6$) in sodium phosphate buffer (10 mM, pH 7.0), NaCl (100 mM), and EDTA (1 mM). Strand concentration = 5 μM.

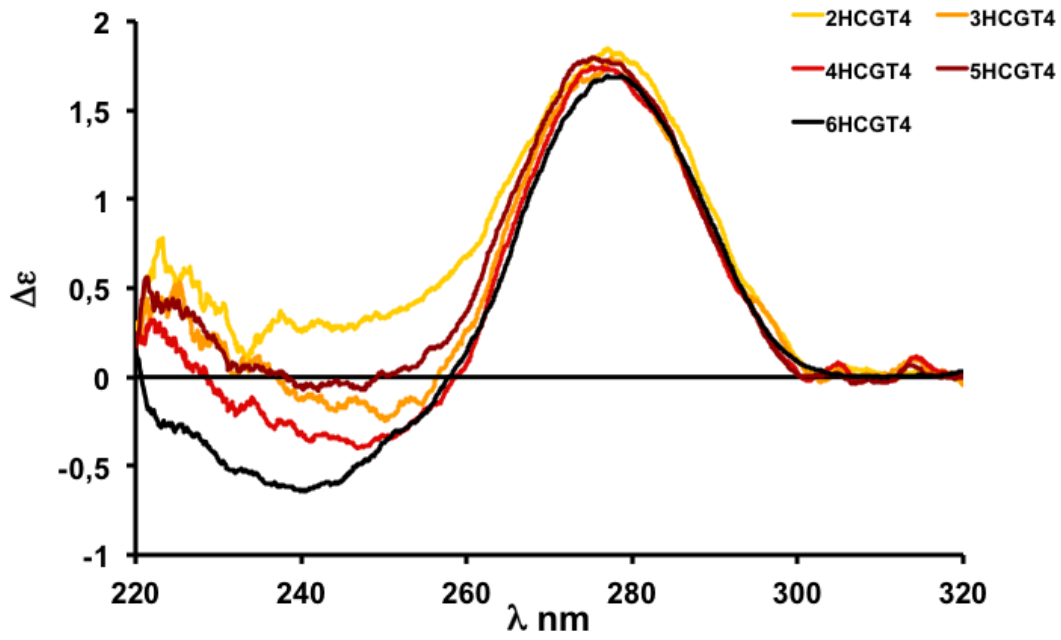

***Figure S8.*** CD spectra at T = 90°C of hairpins $^{i}H_{CG}T_4gp_2$ with stem composed from two to 6 base pairs ($2 \leq i \leq 6$) and with an α,β-D-CNA TT featuring the alpha *gauche*(+) conformation in position 2 within the loop in sodium phosphate buffer (10 mM, pH 7.0), NaCl (100 mM), and EDTA (1 mM). Strand concentration = 5 μM.

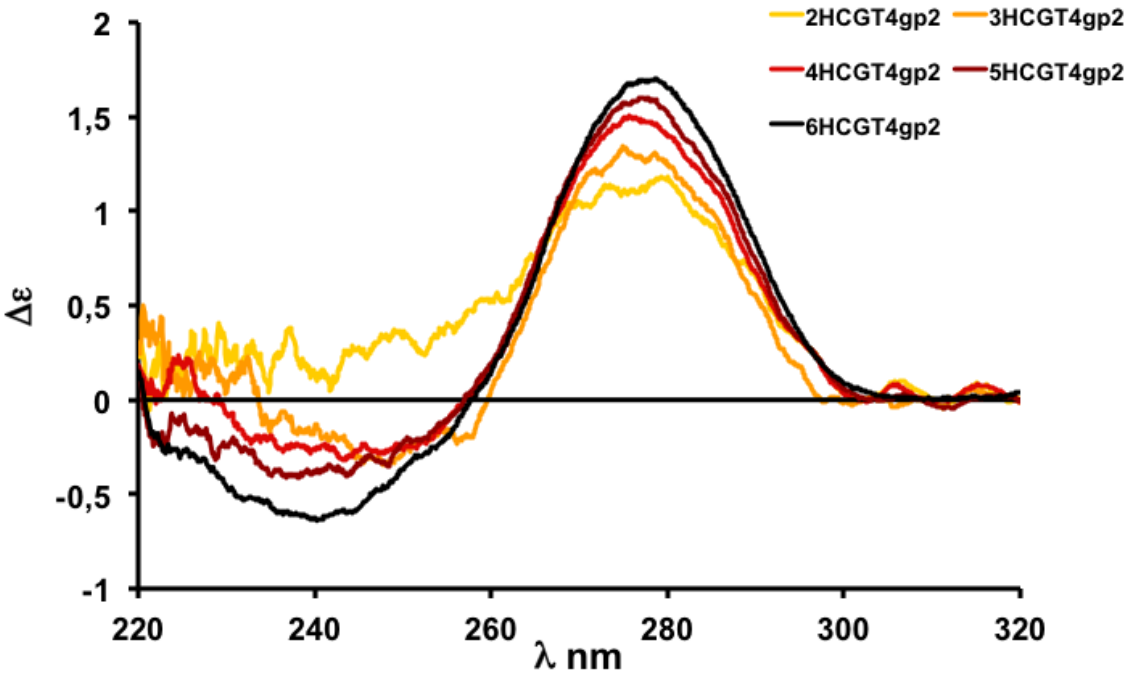


***Figure S9.*** CD spectra at T = 90°C of hairpins $^{i}H_{CG}T_4gp_3$ with stem composed from two to 6 base pairs ($2 \leq i \leq 6$) and with an α,β-D-CNA TT featuring the alpha *gauche*(+) conformation in position 3 within the loop in sodium phosphate buffer (10 mM, pH 7.0), NaCl (100 mM), and EDTA (1 mM). Strand concentration = 5 μM.

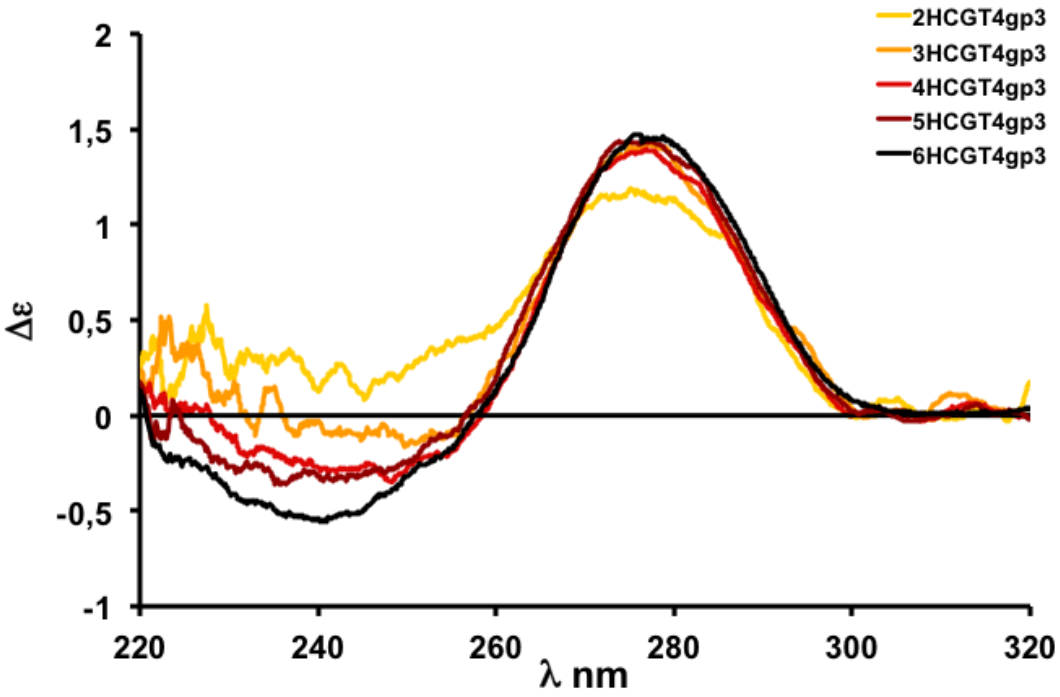

***Figure S10.*** Comparison of CD spectra at T = 25°C of hairpins $^{2}H_{CG}T_4$ (black), $^{2}H_{CG}T_4gp_2$ (red), $^{2}H_{CG}T_4gp_3$ (blue) with stem composed of two base pairs and with an α,β-D-CNA TT featuring the alpha *gauche*(+) conformation in position 2 or 3 within the loop in sodium phosphate buffer (10 mM, pH 7.0), NaCl (100mM), and EDTA (1 mM). Strand concentration = 5 μM.

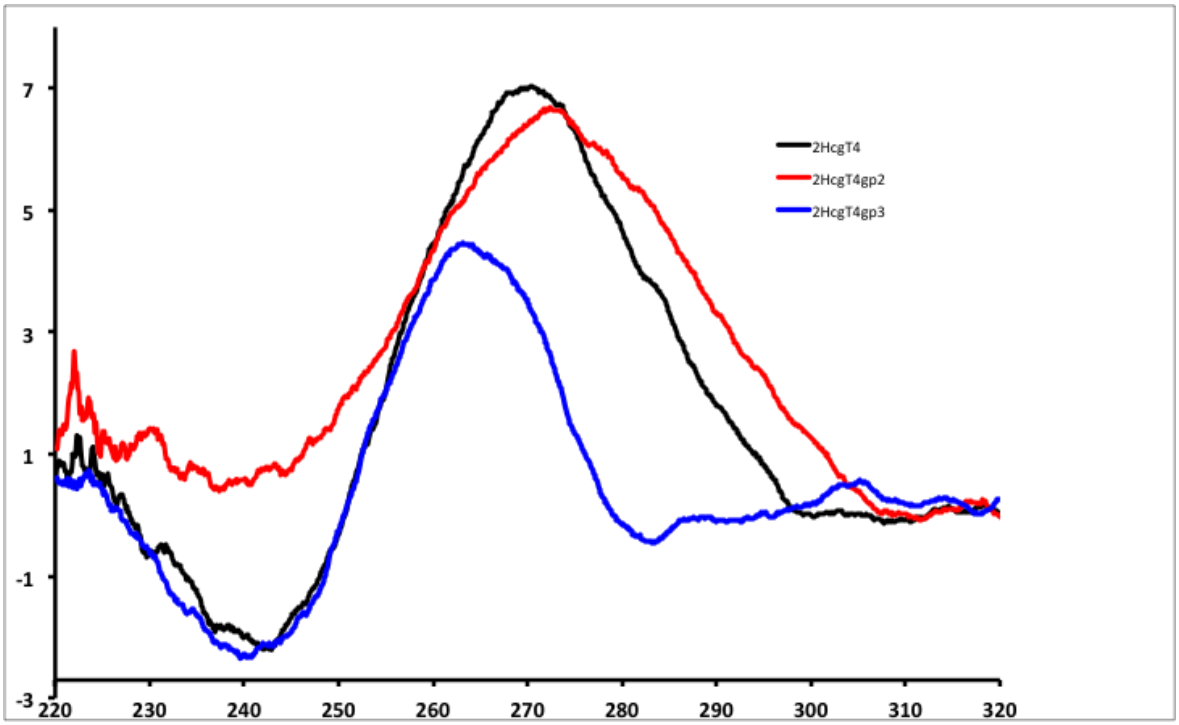


***Figure S11.*** CD spectra of duplexes $H_{AT}$ stem [5'-d(ATCCTA)/5'-d(TAGGAT)] and $H_{CG}$ stem [5'-d(AGGATCC)/5'-d(GGATCCT)] in sodium phosphate buffer (10 mM, pH 7.0), NaCl (100mM), and EDTA (1 mM); T = 5°C. Strand concentration = 5 μM.

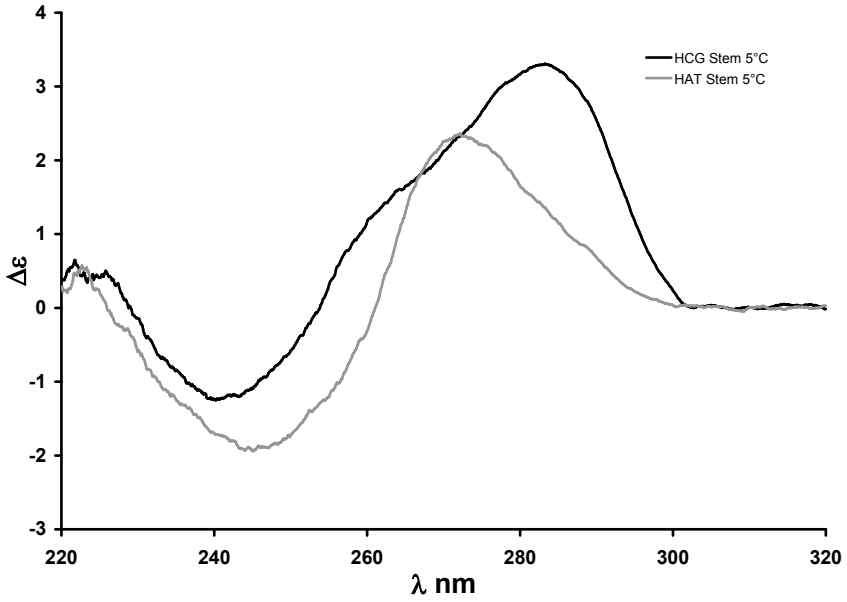

***Figure S12.*** Thermal denaturation curves (Table 3, entry 2), with D-CNA within loop of bulged structures 5'-d(GATTTGCATATxTCATGAG)/3'-d(CTAAACGTATAGTACTC) with x= $PO_2^-$ or dioxaphosphorinane with alpha *gauche*(+) conformation.

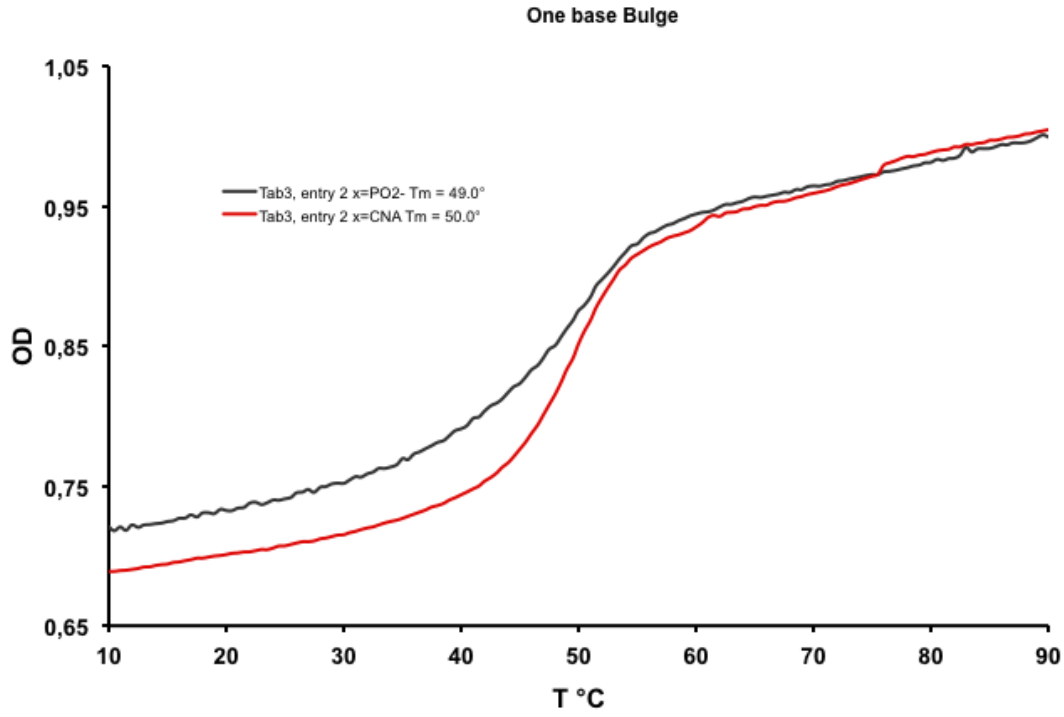


***Figure S12.*** Thermal denaturation curves (Table 3, entry 3), with D-CNA within loop of bulged structures 5'-d(GATTTGCATATxTCATGAG)/3'-d(CTAAACGTATGTACTC) with x= $PO_2^-$ or dioxaphosphorinane with alpha *gauche*(+) conformation.

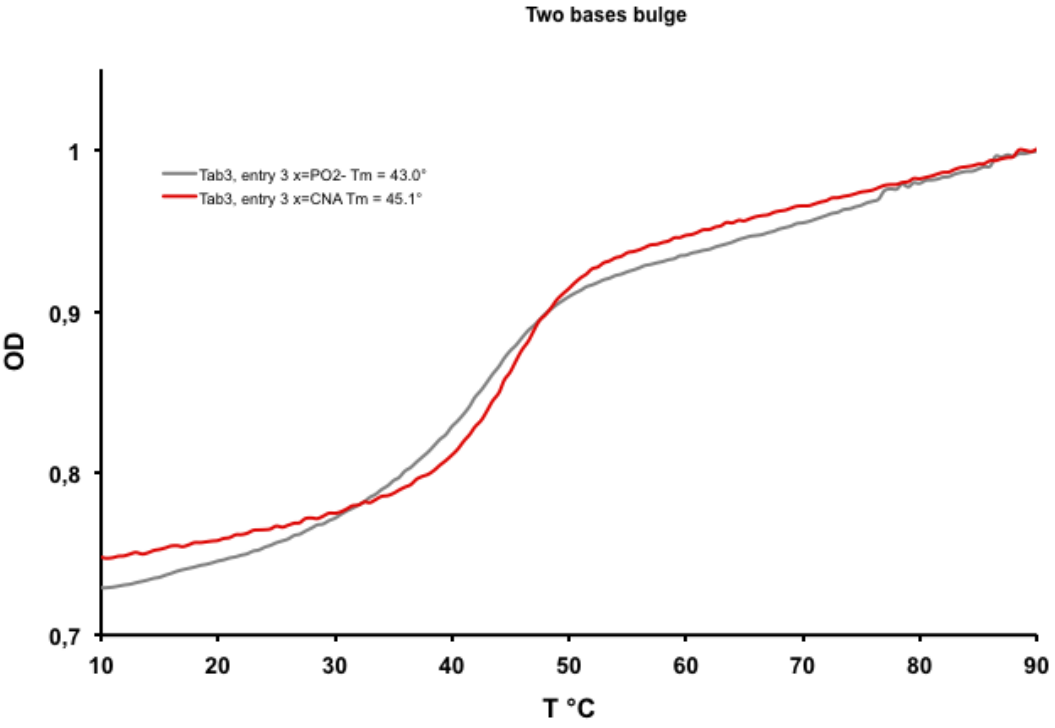

***Figure S13.*** Thermal denaturation curves (Table 3, entry 4), with D-CNA within loop of bulged structures 5'-d(GATTTGCATATxTCATGAG)/3'-d(CTAAACGTAGTACTC) with x= $PO_2^-$ or dioxaphosphorinane with alpha *gauche*(+) conformation.

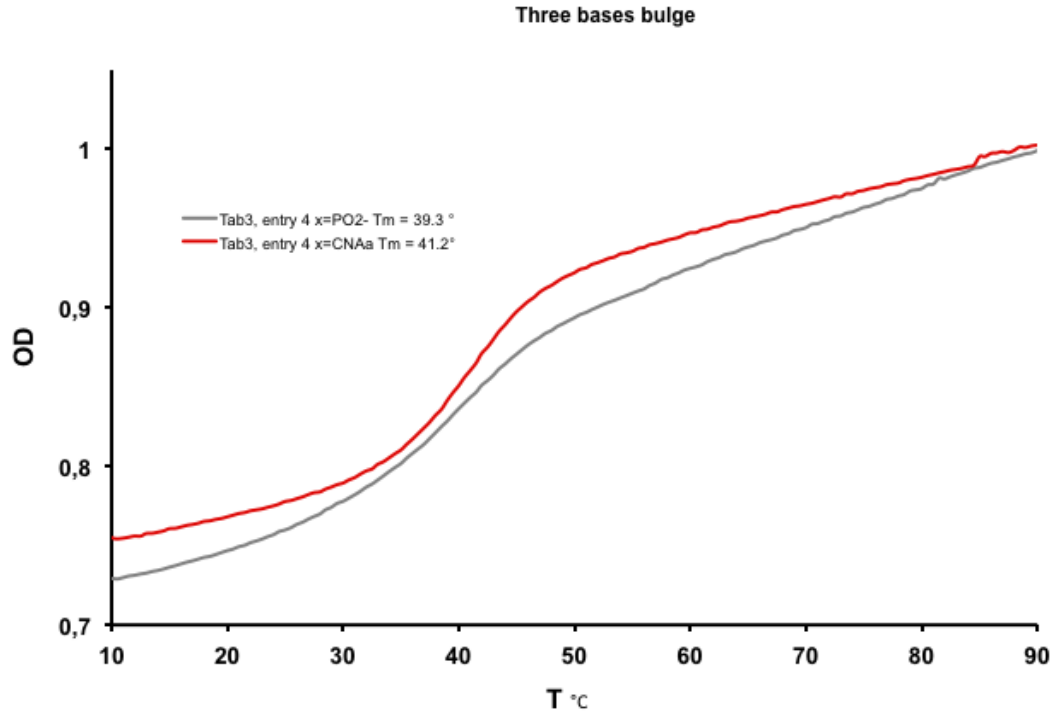


***Figure S14.*** Thermal denaturation curves (Table 3, entry 5), with D-CNA within loop of bulged structures 5'-d(GATTTGCATATxTCATGAG)/3'-d(CTAAACGTATACTC) with x= $PO_2^-$ or dioxaphosphorinane with alpha *gauche*(+) conformation.

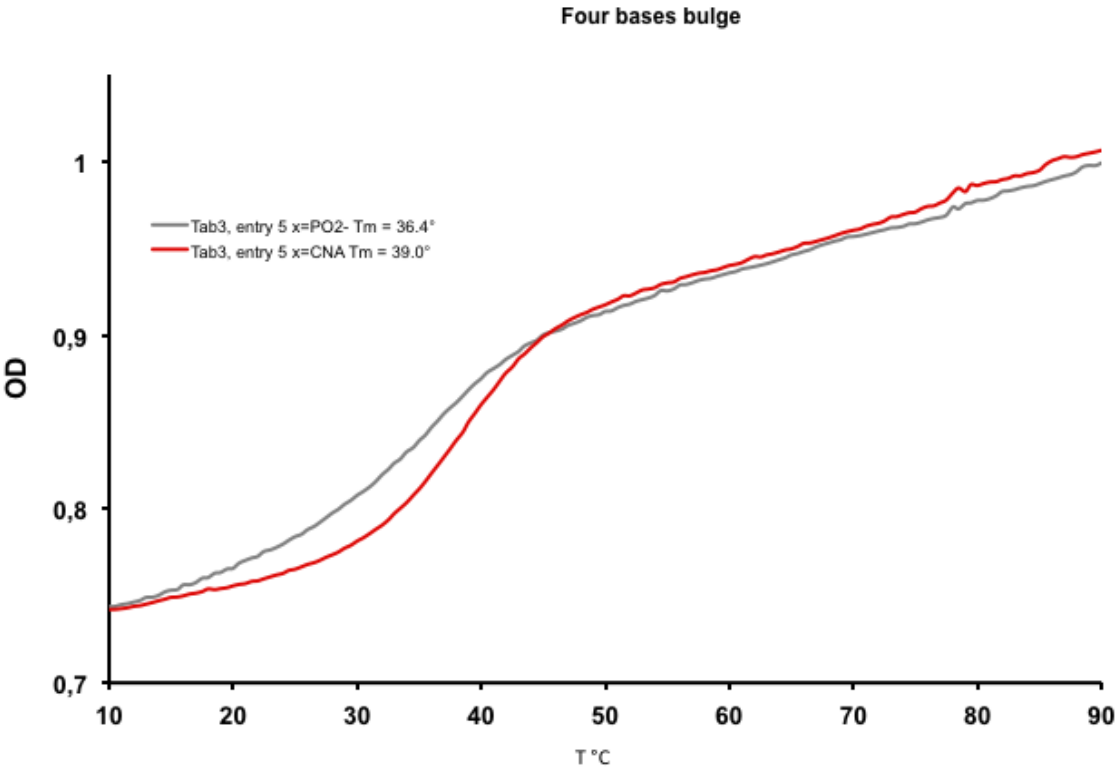

***Figure S15.*** Thermal denaturation curves (Table 3, entry 6), with D-CNA within loop of bulged structures 5'-d(GATTTGCATATxTCATGAG)/3'-d(CTAAACGTTACTC) with x= $PO_2^-$ or dioxaphosphorinane with alpha *gauche*(+) conformation.

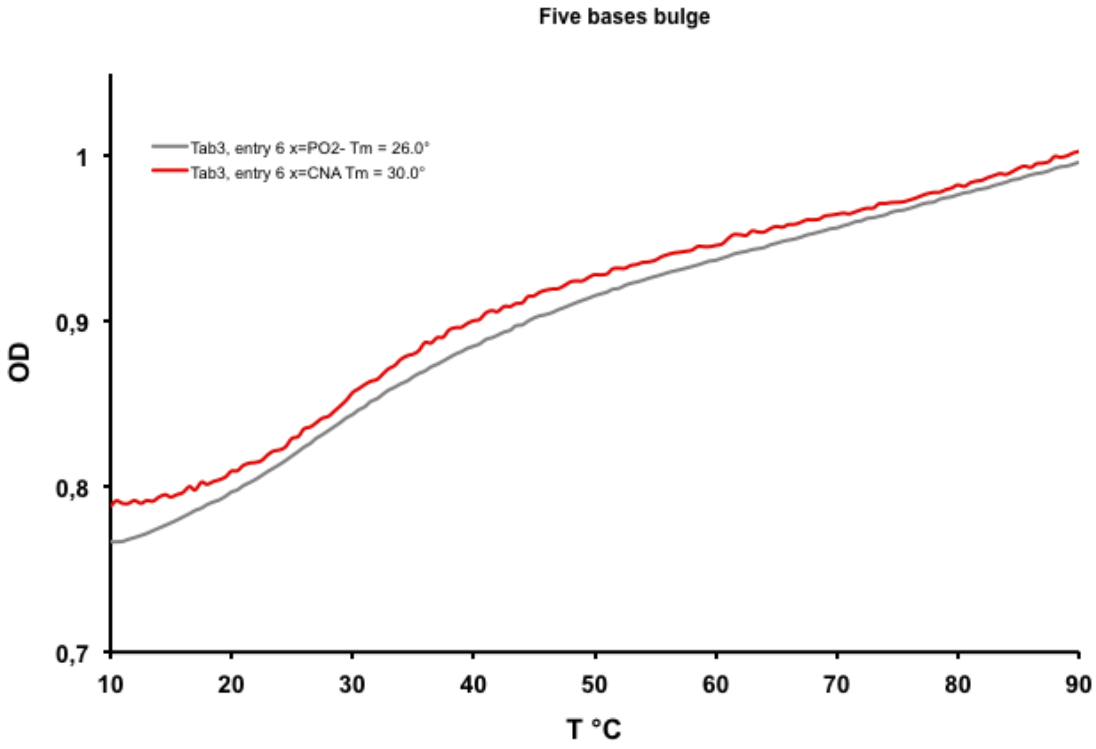


***Figure S16.*** Thermal denaturation curves (Table 3, entry 7), with D-CNA within loop of bulged structures 5'-d(GATTTGCATATxTCATGAG)/3'-d(CTAAACGTACTC) with x= $PO_2^-$ or dioxaphosphorinane with alpha *gauche*(+) conformation.

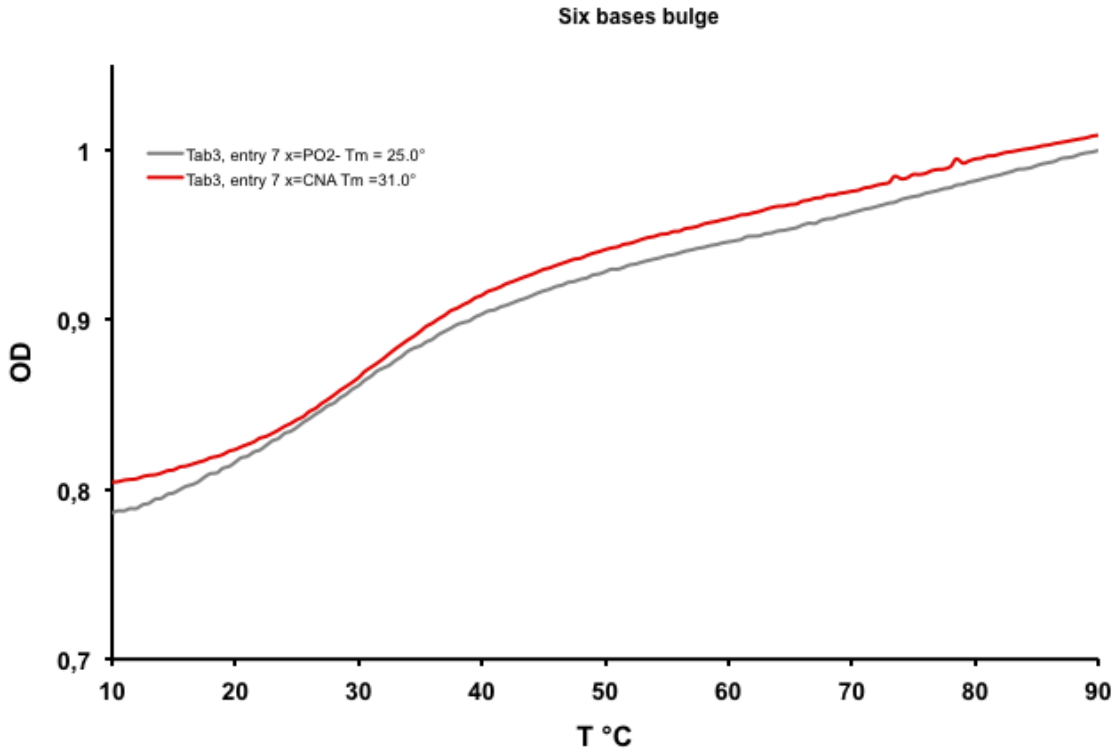


***Figure S17.*** Thermal denaturation curves (Table 4, entry 1), with D-CNA opposite to the loop in bulged structures 5'-d(GATTTGCATATxTCATGAG)/3'-d(CTAAACGTA*T*ATAGTACTC) with x= $PO_2^-$ or dioxaphosphorinane with alpha *gauche*(+) conformation and *T* unpaired nucleotide within the loop.

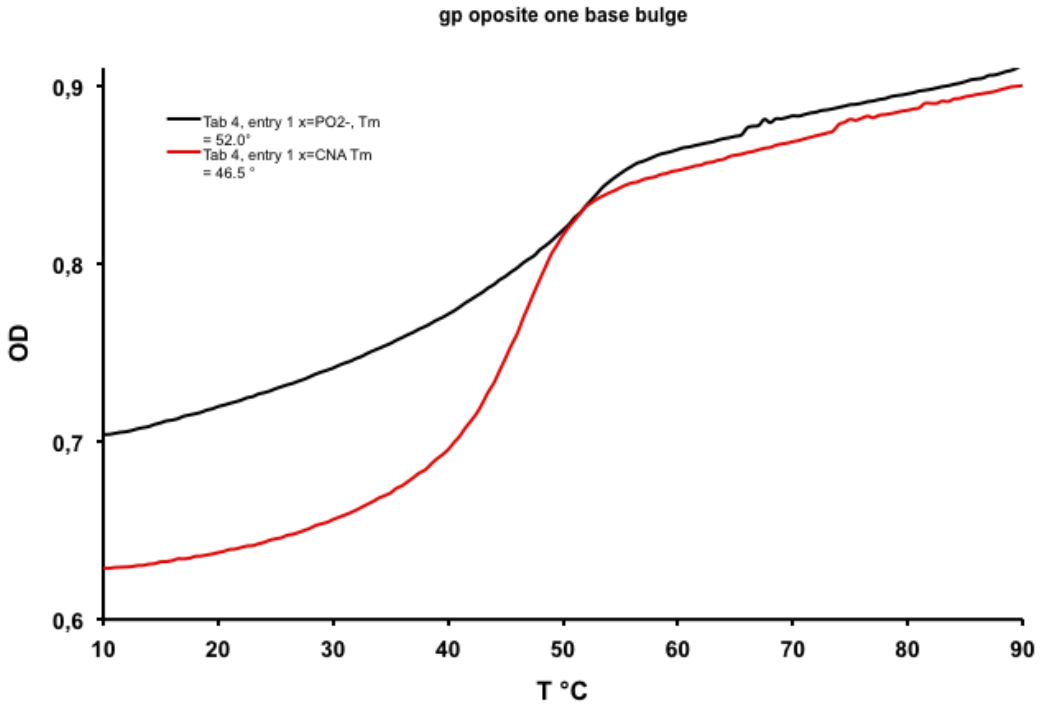


***Figure S18.*** Thermal denaturation curves (Table 4, entry 2), with D-CNA opposite to the loop in bulged structures 5'-d(GATTTGCATATxTCATGAG)/3'-

d(CTAAACGTA*TC*ATAGTACTC) with x= $PO_2^-$ or dioxaphosphorinane with alpha *gauche*(+) conformation and *TC* unpaired nucleotides within the loop.

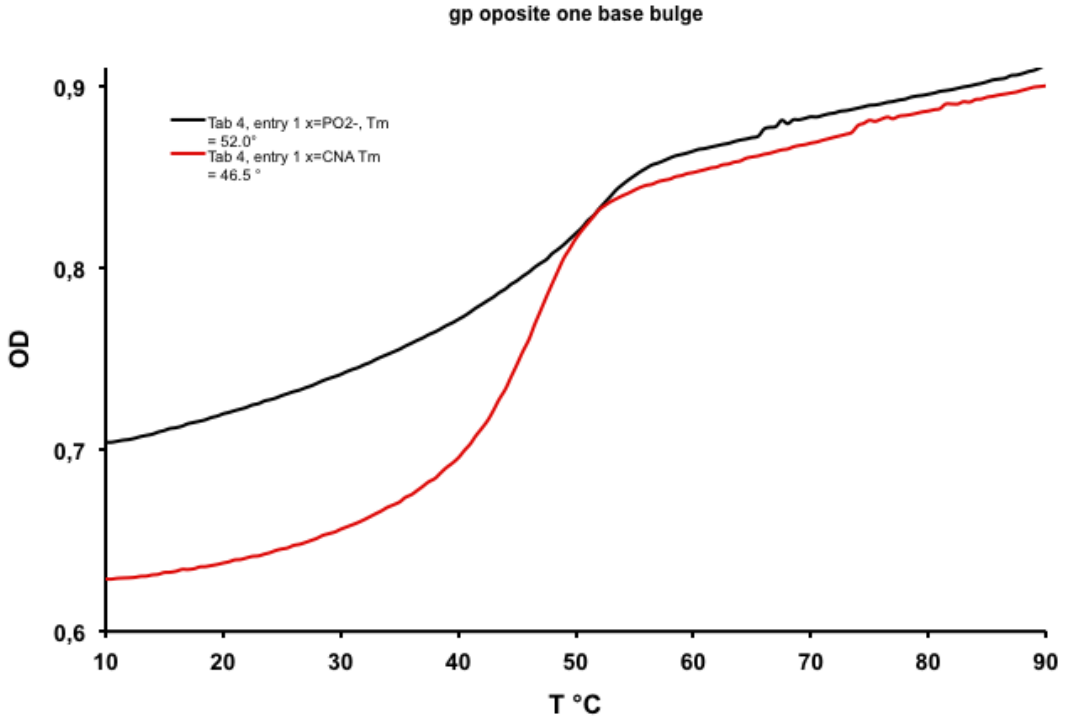


***Figure S19.*** Thermal denaturation curves (Table 4, entry 3), with D-CNA opposite to the loop in bulged structures 5'-d(GATTTGCATATxTCATGAG)/3'-d(CTAAACGTA*TCT*ATAGTACTC) with x= $PO_2^-$ or dioxaphosphorinane with alpha *gauche*(+) conformation and *TCT* unpaired nucleotides within the loop.

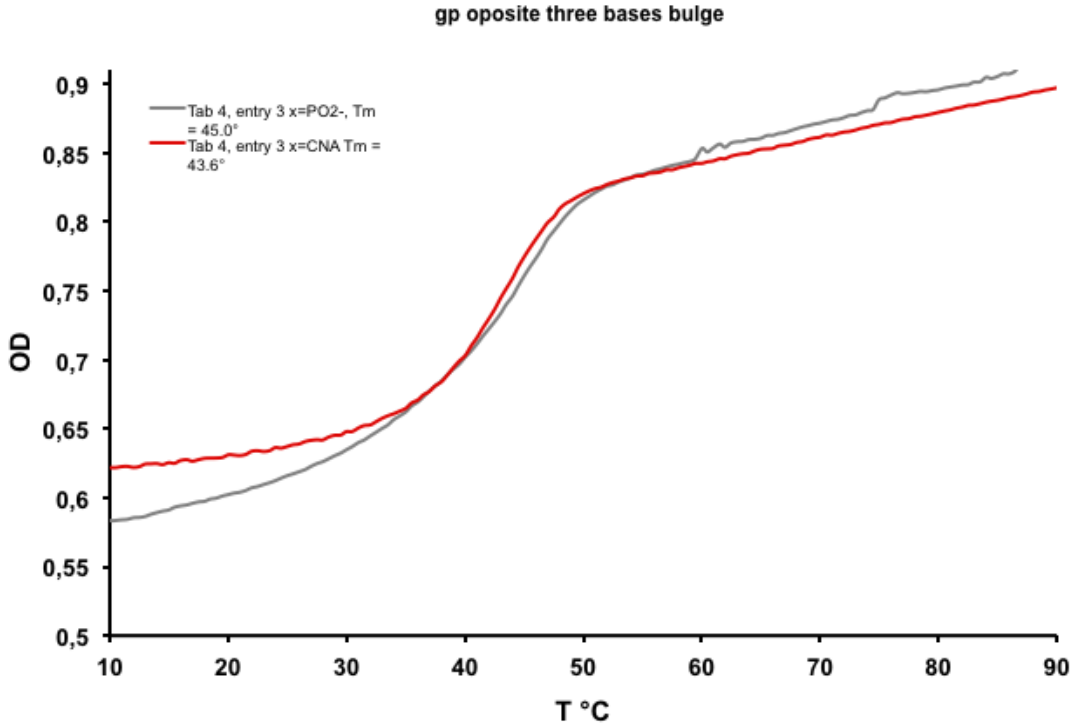


***Figure S21.*** Thermal denaturation curves (Table 4, entry 4), with D-CNA opposite to the loop in bulged structures 5'-d(GATTTGCATATxTCATGAG)/3'-

d(CTAAACGTA*TCTC*ATAGTACTC) with x= $PO_2^-$ or dioxaphosphorinane with alpha *gauche*(+) conformation and *TCTC* unpaired nucleotides within the loop.

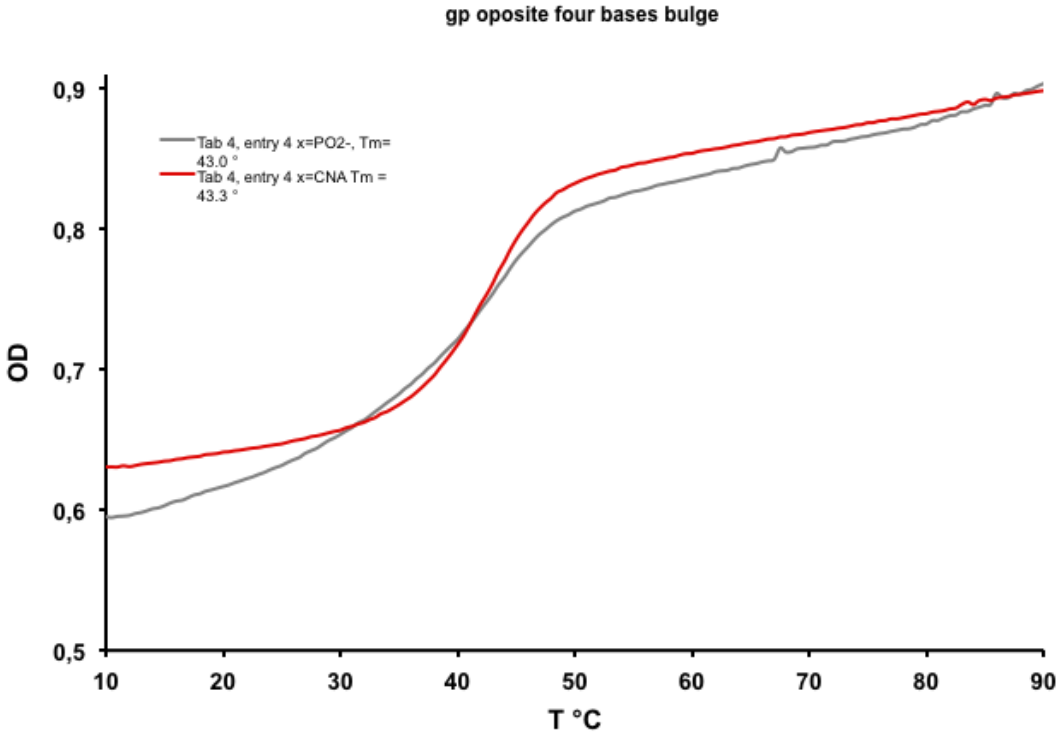


***Figure S22.*** Thermal denaturation curves (Table 4, entry 5 and 6), with D-CNA opposite to the loop in bulged structures 5'-d(GATTTGCATATxTCATGAG)/3'-d(CTAAACGTA*TCTCT*ATAGTACTC) and 5'-d(GATTTGCATATxTCATGAG)/3'-d(CTAAACGTA*TCTCTC*ATAGTACTC) with x= $PO_2^-$ or dioxaphosphorinane with alpha *gauche*(+) conformation and *TCTCT* or *TCTCTC* unpaired nucleotides within the loop.

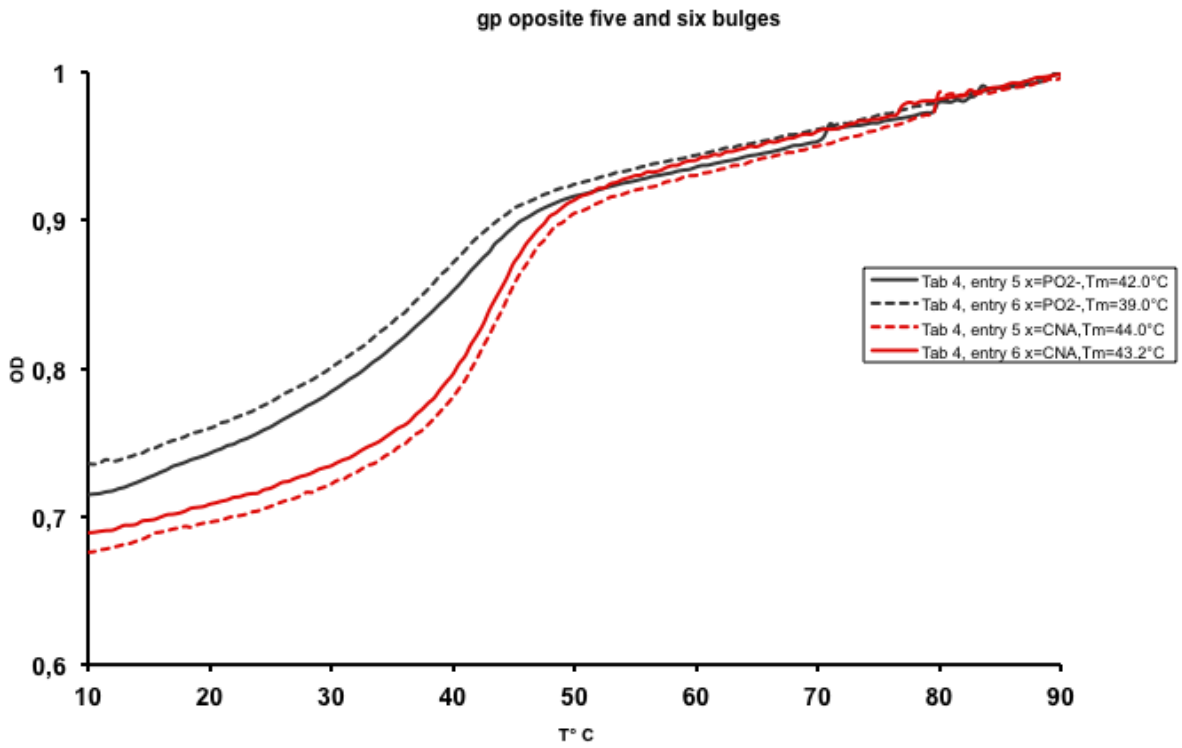
gp oposite five and six bulges
1
0,9
0,8
0,7
0,6
OD
10
20
30
40
50
60
70
80
90
T° C
Tab 4, entry 5 x=PO2-,Tm=42.0°C
Tab 4, entry 6 x=PO2-,Tm=39.0°C
Tab 4, entry 5 x=CNA,Tm=44.0°C
Tab 4, entry 6 x=CNA,Tm=43.2°C